Alzheimer's & Dementia: Diagnosis, Assessment & Disease Monitoring 10 (2018) 583-594

Neuroimaging

A multivariate metabolic imaging marker for behavioral variant frontotemporal dementia

Amir Nazem[a,b,*], Chris C. Tang[b], Phoebe Spetsieris[b], Christian Dresel[b], Marc L. Gordon[c,d], Janine Diehl-Schmid[e], Timo Grimmer[e], Igor Yakushev[f,g], Paul J. Mattis[b], Yilong Ma[b], Vijay Dhawan[b], David Eidelberg[b], for the Alzheimer's Disease Neuroimaging Initiative[1]

[a]*Elmezzi Graduate School of Molecular Medicine, Manhasset, NY, USA*
[b]*Center for Neurosciences, The Feinstein Institute for Medical Research, Manhasset, NY, USA*
[c]*Department of Neurology, Northwell Health, Manhasset, NY, USA*
[d]*Litwin-Zucker Research Center for the Study of Alzheimer's Disease, The Feinstein Institute for Medical Research, Manhasset, NY, USA*
[e]*Department of Psychiatry and Psychotherapy, Klinikum rechts der Isar, Technical University of Munich, Munich, Germany*
[f]*Department of Nuclear Medicine, Klinikum rechts der Isar, Technical University of Munich, Munich, Germany*
[g]*TUM Neuroimaging Center, Klinikum rechts der Isar, Technical University of Munich, Munich, Germany*

Abstract

Introduction: The heterogeneity of behavioral variant frontotemporal dementia (bvFTD) calls for multivariate imaging biomarkers.

Methods: We studied a total of 148 dementia patients from the Feinstein Institute (Center-A: 25 bvFTD and 10 Alzheimer's disease), Technical University of Munich (Center-B: 44 bvFTD and 29 FTD language variants), and Alzheimer's Disease Neuroimaging Initiative (40 Alzheimer's disease subjects). To identify the covariance pattern of bvFTD (behavioral variant frontotemporal dementia–related pattern [bFDRP]), we applied principal component analysis to combined 18F-fluorodeoxyglucose–positron emission tomography scans from bvFTD and healthy subjects. The phenotypic specificity and clinical correlates of bFDRP expression were assessed in independent testing sets.

Results: The bFDRP was identified in Center-A data (24.1% of subject × voxel variance; $P < .001$), reproduced in Center-B data ($P < .001$), and independently validated using combined testing data (receiver operating characteristics–area under the curve = 0.97; $P < .0001$). The expression of bFDRP was specifically elevated in bvFTD patients ($P < .001$) and was significantly higher at more advanced disease stages ($P = .035$:duration; $P < .01$:severity).

Discussion: The bFDRP can be used as a quantitative imaging marker to gauge the underlying disease process and aid in the differential diagnosis of bvFTD.

Keywords: Behavioral variant frontotemporal dementia; Spatial covariance pattern; Differential diagnosis; Quantitative imaging biomarker; FDG PET

Dr. Eidelberg serves on the scientific advisory board and has received honoraria from The Michael J. Fox Foundation for Parkinson's Research; is listed as coinventor of patents, re: Markers for use in screening patients for nervous system dysfunction and a method and apparatus for using same, without financial gain; and has received research support from the NIH (NINDS, NIDCD, and NIAID) and the Dana Foundation. All other authors have declared that no conflict of interest exists.

[1]Some of the data used in preparation of this article were obtained from the Alzheimer's Disease Neuroimaging Initiative (ADNI) database (adni.loni.usc.edu). As such, the investigators within the ADNI contributed to the design and implementation of ADNI and/or provided data but did not participate in analysis or writing of this report. A complete listing of ADNI investigators can be found at http://adni.loni.usc.edu/wp-content/uploads/how_to_apply/ADNI_Acknowledgement_List.pdf.

*Corresponding author. Tel.: +(516) 562-1204; Fax: +(516) 562-1008.
E-mail address: anazem@northwell.edu

https://doi.org/10.1016/j.dadm.2018.07.009

1. Introduction

Behavioral variant frontotemporal dementia (bvFTD) is the most common clinical phenotype of frontotemporal lobar degeneration (FTLD), a leading cause of dementia in midlife [1]. This syndrome is characterized by progressive impairment of personal and social behavior, as well as emotional, language, and executive functions [1]. However, similar symptoms are also seen in various other psychiatric and neurodegenerative disorders, particularly Alzheimer's disease (AD), making accurate diagnosis of bvFTD challenging [1], especially at early stages of the disease [2].

Overall, the accuracy of clinical diagnosis of dementia has been improved with the study of ^{18}F-fluorodeoxyglucose (FDG) positron emission tomography (PET) brain scans [3], as suggested by the diagnostic criteria for bvFTD [4] and AD [5]. However, the considerable individual variability in neuroanatomical involvement seen in bvFTD patients [6–8] restricts the use of regional and univariate analytical approaches for early and accurate detection of this disorder [2,7,9], calling for the identification and standardization of multivariate quantitative imaging biomarkers [10,11] for this dementia syndrome [12].

A multivariate brain mapping approach, based on principal component analysis (PCA), has been applied to FDG PET data for several neurodegenerative disorders to identify disease-related spatial covariance patterns [13–15]. The expression of such metabolic signatures [10,13] can be quantified in the scan data of prospective individual subjects [14,15] and thus has been used to aid in early differential diagnosis, predict disease progression, and track response to therapy [13].

Nonetheless, to date, a metabolic covariance pattern has not been determined for bvFTD. The main objective of this study was to identify and characterize the bvFTD metabolic covariance pattern (bvFTD-related pattern [bFDRP]) and assess its performance as an imaging marker for bvFTD. Our basic hypothesis was that bFDRP can classify independent bvFTD patients from healthy controls. Specifically, we identified bFDRP in a North American sample, cross-validated its reproducibility in a pathology-confirmed European sample, and assessed its clinical correlates and classification performance for early-stage dementia.

2. Methods

2.1. Participants

Data were collected consecutively for dementia patients who had been referred for FDG PET scanning either to the Feinstein Institute for Medical Research in Manhasset, NY, (called Center-A) between 2000 and 2014 or to the Technical University of Munich in Munich, Germany, (called Center-B) between 1999 and 2008. Ethical permission for the studies was obtained from the Institutional Review Board of Center-A and the Ethics Commission of Center-B, which also granted a waiver of consent for all subjects.

Before the identification of bFDRP, a retrospective chart review was performed to determine the patient enrollment based on published clinical criteria for the corresponding disorders (i.e., bvFTD [4], AD [5], semantic dementia [SD], and progressive nonfluent aphasia [PNFA] [16]). Enrolled subjects for this study included a total of 35 patients scanned at Center-A (25 bvFTD and 10 AD), 73 patients scanned at Center-B (44 bvFTD, 17 SD, and 12 PNFA), and 40 AD subjects randomly retrieved from the Alzheimer's Disease Neuroimaging Initiative (ADNI) database (adni.loni.usc.edu; see www.adni-info.org; previously studied at Center-A [17]). Table 1 summarizes the demographic information of participants.

Center-A training set included the probable bvFTD patients for whom long-term clinical follow-up were available (n = 10). Center-B training set included definite bvFTD patients with autopsy or genetic evidence for FTLD pathology (n = 7). The rest of patients were used as testing data. We also used scan data of 80 age-matched healthy volunteers as control groups (NL). Fig. 1 demonstrates the study design.

We applied the epidemiological evidence of an average 3.5 years of delay in diagnosis of bvFTD [18] and AD [19] as a cutoff point to identify subjects at early stage of dementia. Subjects who had short symptom duration at FDG PET

Table 1
Demographics

Center	Group	Number (M/F)	Age at PET scan (years)	Symptom duration (years)
A	Training			
	NL	10 (8/2)	71.3 ± 6.5	-
	bvFTD	10 (8/2)	72.1 ± 9.7	3 ± 1.9
	Testing			
	NL	15 (5/10)	68.7 ± 6.3	-
	bvFTD	15 (8/7)	69.7 ± 11.2	3.1 ± 1.7
	AD	10 (6/4)	70.2 ± 5.8	3.2 ± 2.2
B	Training			
	NL*	15 (7/8)	61.8 ± 9.1	-
	bvFTD	7 (7/0)	60.1 ± 12.1	4.1 ± 4.4
	Testing			
	bvFTD	37 (28/9)	63.7 ± 8.9	3.5 ± 2.8
	SD	17 (11/6)	65.5 ± 4.3	3.8 ± 2.1
	PNFA	12 (6/6)	70.2 ± 8.9	3.5 ± 1.8
ADNI	Testing			
	NL	40 (23/17)	75.8 ± 4.64	-
	AD	40 (23/17)	75.7 ± 5.76	4.4 ± 2.6

Abbreviations: AD, Alzheimer's disease; ADNI, Alzheimer's Disease Neuroimaging Initiative; bvFTD, behavioral variant frontotemporal dementia; NL, healthy controls; PNFA, progressive nonfluent aphasia; SD, semantic dementia.

NOTE. Data are mean ± standard deviation.

*NL group from Center-B was used both in training and testing analysis.

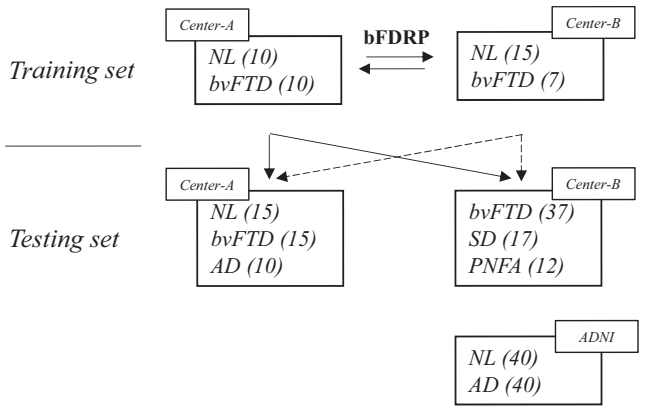

Fig. 1. Study design: A total of 148 dementia subjects and 80 healthy controls were studied. Subjects were grouped based on data source, dementia cause, or diagnostic certainty. Subjects scanned at Center-A (*left*) included 25 bvFTD and 10 AD patients. Long-term clinical follow-up information was available for the 10 bvFTD subjects used in Center-A's training set for the identification of bFDRP. Subjects scanned at Center-B (*right*, top two boxes) included 44 bvFTD, 17 SD, and 12 PNFA patients. Seven bvFTD subjects scanned at Center-B had pathological confirmation of FTLD and were used in a training set to assess topographical reproducibility of bFDRP. In addition, we used 40 AD subjects retrieved randomly from ADNI. Testing sets have been used for assessing disease relatedness, classification performance, or clinical correlates of bFDRP. Abbreviations: AD, Alzheimer's disease; ADNI, Alzheimer' Disease Neuroimaging Initiative; bvFTD, behavioral variant frontotemporal dementia; bFDRP, behavioral variant frontotemporal dementia–related pattern; FTLD, frontotemporal lobar degeneration; NL, healthy controls; PNFA, progressive nonfluent aphasia; SD, semantic dementia.

scanning (<3.5 years) but had moderate-to-severe cognitive (Mini–Mental Status Examination [MMSE] < 19) or functional impairment (Clinical Dementia Rating [CDR] score > 1) were not included for early-stage classification analyses.

2.2. Positron emission tomography

For Center-A subjects, FDG PET imaging was performed within 2 months of clinical diagnosis (19 ± 15 days) on a GE Advance tomograph (General Electric, Milwaukee, WI) as described previously [20]. Center-B subjects were scanned with FDG PET within 14 days of clinical diagnosis using the Siemens ECAT HR+ tomograph (CTI, Knoxville, TN) at that institution [21]. Similarly, for ADNI subjects, FDG PET scanning was performed within 14 days of the clinical diagnosis (www.adni-info.org).

2.3. Image analysis

All scans were reoriented to MNI coordinate space, spatially normalized to a standard PET brain template, and smoothed with a three-dimensional gaussian kernel (full-width at half-maximum = 8 mm) [22], using SPM5 (Wellcome Trust Centre for Neuroimaging, Institute of Neurology, London, UK) running on Matlab 7.3 (MathWorks Inc., Natick, MA). The preprocessed scans were then analyzed for pattern identification (Section 2.3.1) and quantification (Section 2.3.2) [14] using a MATLAB-based software freely available at https://feinsteinneuroscience.org/imaging-software.

2.3.1. Pattern identification

For pattern identification, a PCA was performed on the FDG PET scan data from Center-A's training group that consisted of 10 bvFTD patients and 10 age-matched NL subjects (see Fig. 1 and Table 1). Of note, to identify the candidate disease-related brain pattern, a healthy control group should be included in the PCA training set. The use of healthy control group in the training set facilitates isolation and detection of the discriminant features of data structure. Refer to references [14,15] for further methodological details. Cattell's scree plot was used to assess the contribution of each principal component (PC) to the total subject × voxel variance (cf. Supplementary Fig. 1) [14,23]. All subjects express each of these PCs by a corresponding score that is used to identify the PCs that contain significant disease-related information [14,15]. We used a criterion of $P < .05$ (Student's *t*-test) to identify PCs whose scores discriminated patients from controls in the training group [14,23]. If more than one PC was significant, a linear combination of PCs could be considered [23]. The selected disease-related topography was termed bvFTD-related pattern (bFDRP). The validity of the pattern was further examined by its ability to discriminate independent testing groups of bvFTD patients and healthy controls based on their pattern expression scores [14,15,23]. Center-A training subjects were not used in any prospective analyses involving Center-A–derived bFDRP.

2.3.2. Pattern expression

The expression of bFDRP was quantified in all testing FDG PET scans obtained from Center-A, Center-B, or the ADNI (see Fig. 1 and Table 1). This was performed on a prospective single-case basis using a voxel-based algorithm blind to subject diagnostic category and group membership (https://feinsteinneuroscience.org/imaging-software) [14].

In summary, subject score (SS) of bFDRP expression in an individual FDG PET scan (*i*) is computed by the inner product of the bFDRP vector and the corresponding subject residual profile (SRP_i) vector ($SS_i = SRP_i$. bFDRP) [14,15,23]. As previously explained in further details [14,15,23], for each scan, the subject residual profile vector is computed by voxelwise removal of the scan mean value and the reference group mean value for each corresponding voxel.

All pattern expression values were standardized (*z*-scored) with respect to corresponding measures from

the Center-A healthy control group that was used for the identification of bFDRP.

2.4. Disease relatedness, classification, and clinical correlates

We examined the disease relatedness of bFDRP by computing its expression in independent testing cohorts from Center-A (15 probable bvFTD versus 15 NL) and Center-B (seven definite bvFTD and 37 probable bvFTD versus 15 NL) [14,15,23].

To evaluate phenotypic specificity of bFDRP, we computed its expression for patients with AD (scanned at Center-A or retrieved from ADNI) or FTD language variants (i.e., patients with SD and PNFA scanned at Center-B) (Table 1). Single-case discriminations between bvFTD and other disease categories were performed on all testing data using bFDRP expression values (cf. Section 2.6).

To assess the clinical correlates of bFDRP, we compared its expression between bvFTD subgroups categorized based on symptom duration (*early* vs. *late*) or severity of functional impairment as determined by CDR global scores. Correlation analyses were also performed between bFDRP expression values and the aforementioned variables.

2.5. Reproducibility of bFDRP topography

To assess the reproducibility of bFDRP, we applied the same method explained in Section 2.3.1 to Center-B's training set consisting of the seven bvFTD patients with FTLD pathology and their age-matched control group (n = 15; see Table 1). For validation, the expression of this pattern was quantified in the scan data of independent testing samples from both centers. Clinical correlates of $bFDRP_B$ were assessed using the method explained in Section 2.4. Spatial relationship between the bFDRP topographies from the two centers was evaluated by voxelwise correlation analysis incorporating a correction for spatial autocorrelation [24]. The relationship between expression values for the two topographies was assessed in bvFTD testing data using Pearson's correlation.

2.6. Statistical analysis

Standardized bFDRP expression values were compared for bvFTD and healthy control data using Student's *t*-tests, and across groups from each site using one-way ANOVA with post hoc Dunnett's test. These analyses were performed using SPSS 9.0 (SPSS Inc., Chicago, IL) and were considered significant for $P < .05$, corrected for multiple comparisons. Logistic regression analysis was used for classification at the single-case level. Classification performance was determined through receiver operating characteristics curve analysis using MedCalc17.9. The optimal diagnostic cutoff value was identified for the receiver operating characteristics curve coordinate with the greatest Youden's index [25] for a specificity of >80%.

3. Results

3.1. Participants

3.1.1. Center-A

Twenty-five probable bvFTD patients were scanned at Center-A. Ten of these were referred from Center-A–affiliated clinics and had long-term clinical follow-up (19.3 ± 13.6 months), consistent with the diagnosis of bvFTD, and thus were enrolled in the Center-A training set (8 males [M]/2 females [F]; age: 72.1 ± 9.7 years; symptom duration: 3 ± 1.9 years; MMSE: 27.3 ± 2.7). One patient in the training set received a diagnosis of bvFTD with definite FTLD pathology based on autopsy-confirmed TDP-43 proteinopathy. The remaining 15 bvFTD subjects scanned at Center-A were referred from dementia community clinics and were enrolled in the testing set (8 M/7 F; age: 69.7 ± 11.2 years; symptom duration: 3.1 ± 1.7 years; MMSE: 24.7 ± 4; no clinical follow-up; see Fig. 1). Center-A data also included 10 testing patients with probable AD (6 M/4 F; age: 70.2 ± 5.8 years; symptom duration: 3.2 ± 2.2 years; MMSE: 18 ± 6.8), used for assessing the phenotypic specificity of bFDRP, as well as its performance in single-case classification. The 25 healthy volunteers were age-matched to the corresponding bvFTD patients ($P > .8$, Student's *t*-test).

3.1.2. Center-B

Among the 44 bvFTD patients scanned at Center-B, seven patients who had a pathological diagnosis consistent with FTLD (7 M; age: 60.1 ± 12.1 years; symptom duration: 4.1 ± 4.4 years; MMSE: 25.4 ± 3.1) were enrolled in Center-B training set (see Section 3.4).

The remaining 37 bvFTD patients scanned at Center-B, for whom a pathological confirmation was not available, were enrolled in Center-B testing set (28 M/9 F; age: 63.7 ± 8.9 years; symptom duration: 3.5 ± 2.8 years; MMSE: 22.4 ± 4.9). This group could be further divided into "*early*" (n = 23, 17 M/6 F, symptom duration: 1.8 ± 0.8 years) and "*late*" (n = 14,11 M/3 F, symptom duration: 6.5 ± 2.4 years) subgroups based on symptom duration, as well as *very mild* (CDR = 0.5, n = 9), *mild* (CDR = 1, n = 21) and *moderate* (CDR = 2, n = 7) severity subgroups based on CDR global scores (cf. Section 3.3.3). In addition, to assess the phenotypic specificity of bFDRP, we studied subjects with FTD language variants, that is, PNFA (n = 12, 6 M/6 F; age: 70.2 ± 8.9 years; symptom duration: 3.5 ± 1.8 years) and SD (n = 17, 11 M/6 F; age: 65.5 ± 4.3 years; symptom duration: 3.8 ± 2.1 years) all scanned at Center-B. Of note, age was not different between healthy volunteers and the corresponding bvFTD groups from this center ($P > .49$ Student's *t*-test).

3.1.3. Alzheimer's Disease Neuroimaging Initiative

We used the baseline FDG PET scans of 40 AD subjects, drawn randomly from the ADNI database (23 M/17 F; age: 75.7 ± 5.76 years; symptom duration: 4.4 ± 2.6 years; MMSE: 23.5 ± 2). For control analysis, a sample of 40 age-matched healthy volunteers was also downloaded from ADNI.

3.2. Pattern identification

Spatial covariance analysis of metabolic scan data from Center-A's training set (10 bvFTD and 10 age-matched NL, data combined) revealed that the first principal component (PC1), accounting for 24.1% of the subject × voxel variance, could separate bvFTD patients from healthy volunteer subjects ($P < .001$; permutation test, 500 iterations; Fig. 2A). The subsequent PCs (Supplementary Fig. 1), however, did not contribute to the discrimination between patients and healthy controls ($P > .16$). Hence, PC1 was recognized as the bFDRP. The topographical features of bFDRP are reported in Fig. 2B and Section 3.5.

3.3. Pattern expression

3.3.1. Disease relatedness

The disease relatedness of bFDRP was validated in independent bvFTD testing samples from both centers (15 probable bvFTD patients scanned at Center-A; seven definite and 37 probable bvFTD patients scanned at Center-B). The bFDRP expression was elevated in testing bvFTD patients from both centers relative to the corresponding healthy control subjects ($P < .001$; Student's t-tests) and could separate the seven definite bvFTD patients from the corresponding healthy controls (see Fig. 3). Of note, bFDRP expression values were comparable between the definite and probable bvFTD patients ($P > .15$). Pattern expression was not different between the three independent control groups ($P > .2$, Student's t-tests).

Receiver operating characteristics curve analysis of the individual data revealed excellent separation of combined testing bvFTD patients and control subjects from both sites (area under the curve = 0.977, $P < .0001$; Table 2, Fig. 4A). Similar classification outcome was achieved when the analysis was only performed between testing subjects at the early stage of bvFTD (n = 31; cf. Section 2.1) and healthy controls (area under the curve = 0.976, $P < .0001$).

3.3.2. Disease classification

The bFDRP expression values were markedly lower in AD, SD, and PNFA patients relative to the corresponding bvFTD groups ($P < .001$; post hoc Dunnett's tests, Fig. 3). Although bFDRP expression was marginally increased in PNFA subjects relative to normal ($P = .05$; Student's t-test), corresponding differences did not reach significance for the SD and AD groups ($P > .1$; Fig. 3).

The discriminatory power of bFDRP expression values between all testing bvFTD and AD subjects reached

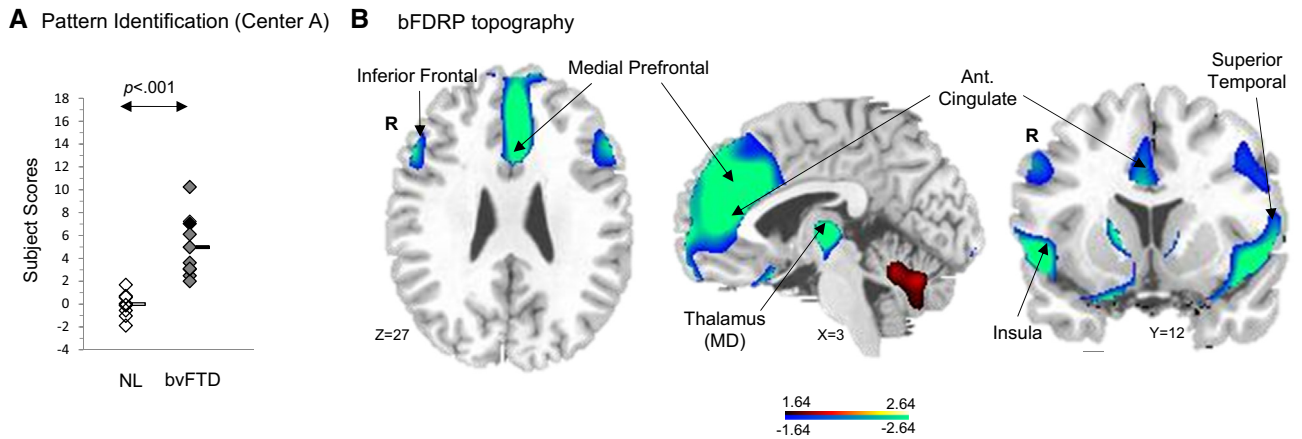

Fig. 2. Behavioral variant frontotemporal dementia–related pattern (bFDRP): (A) Spatial covariance analysis (SSM/PCA) was performed on metabolic PET scans from Center-A's training set, including 10 bvFTD patients with long-term clinical follow-up and 10 age-matched healthy control subjects. The bvFTD subject marked in black had FTLD histopathological evidence consistent with TDP-43. Only the first principal component, accounting for 24.1% of total data variance (cf. Supplementary Fig. 1), contributed to discrimination between patients and NL ($P < .001$; permutation test) and thus was termed bFDRP (Subjects scores are standardized to the reference group used for pattern identification [mean = 0; SD = 1]). (B) The topography of bFDRP was characterized by bilateral metabolic reductions in the medial prefrontal cortex, middle and inferior frontal gyri, anterior cingulate region, superior temporal gyrus, insula, and the mediodorsal (MD) thalamic nucleus, associated with relative metabolic increases in the middle and inferior occipital gyri (not shown) and in the posterior lobe of the cerebellum. (The images are generated by superimposing the candidate topography onto a standard brain template. The displayed regions contributed significantly to the topography at $|z| > 1.64$, $P < .05$ [one-tailed] and demonstrated to be reliable by bootstrap estimation. Regions with positive weights [i.e., covariance metabolism above mean] were color-coded red, whereas those with negative weights [i.e., covariance metabolism below mean] were color-coded blue. The right hemisphere is labeled "R."). Abbreviations: bvFTD, behavioral variant frontotemporal dementia; FTLD, frontotemporal lobar degeneration; NL, healthy controls; PCA, principal component analysis; SSM, scaled subprofile modeling.

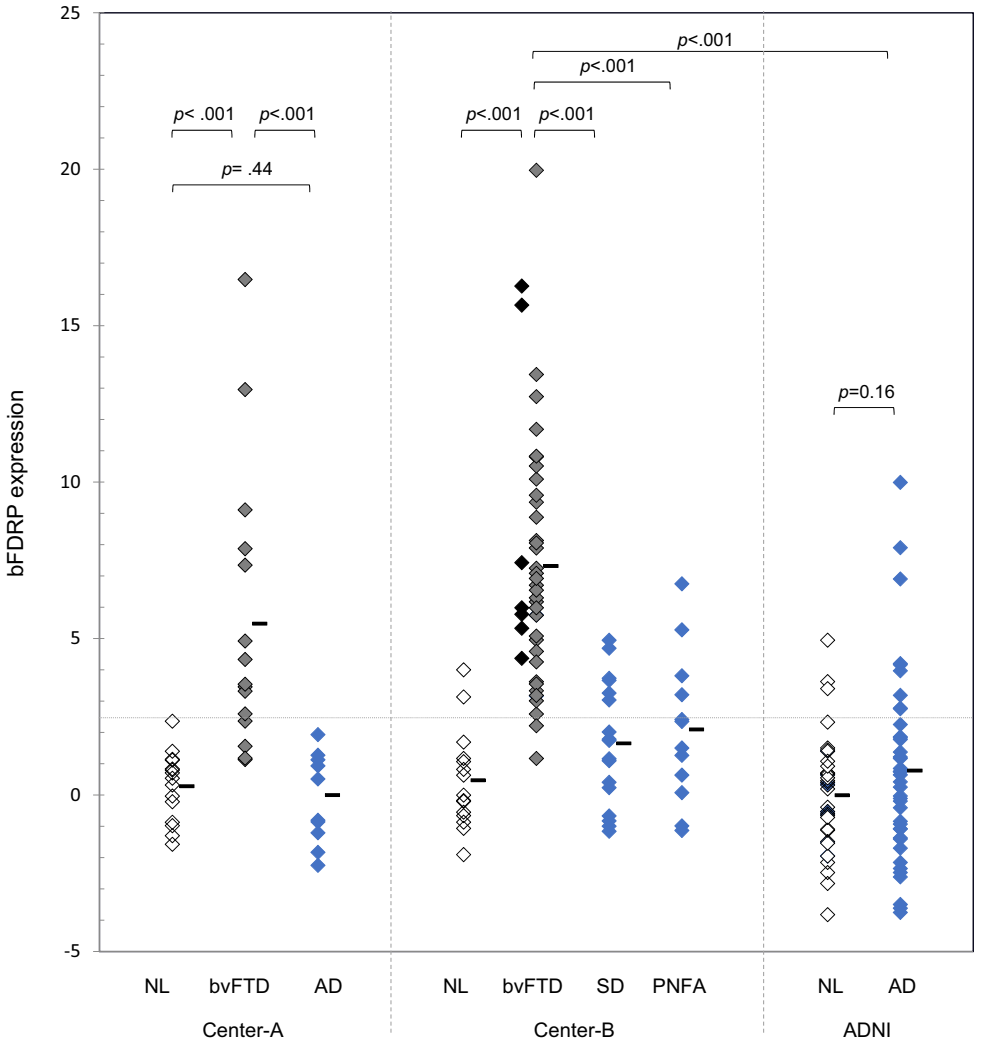

Fig. 3. Pattern expression: Disease relatedness. The bFDRP expression values are displayed for all testing subjects. *Left (Center-A data)*: Pattern expression was significantly elevated in bvFTD patients (n = 15) compared with healthy subjects (n = 15; $P < .001$; Student's *t*-test) and AD patients (n = 10; $P < .001$). AD patients exhibited bFDRP expression levels with no significant difference from normal ($P = .4$). *Middle* (*Center-B data*): Pattern expression in the Center-B bvFTD patients (37 probable and 7 definite bvFTD patients indicated by gray and black diamonds, respectively) was elevated relative to the corresponding NL group and all other disease groups ($P < .001$ for comparisons with *bvFTD*, post hoc Dunnett's tests). Pattern expression was marginally increased in PNFA (n = 12) subjects relative to normal ($P = .05$; Student's *t*-test); corresponding differences did not reach significance for the SD (n = 17; $P > .1$). *Right* (*ADNI data*): Similarly, the expression of bFDRP was not different ($P = .16$) in AD patients (n = 40) retrieved from ADNI compared with their corresponding NL (n = 40). (Pattern expression was standardized to the reference group used for pattern identification. The horizontal dotted line represents the optimal cutoff value for classification between bvFTD and healthy control subjects [cf. Fig. 4A]). Abbreviations: AD, Alzheimer's disease; bvFTD, behavioral variant frontotemporal dementia; bFDRP, behavioral variant frontotemporal dementia–related pattern; NL, healthy controls; PNFA, progressive nonfluent aphasia; SD, semantic dementia.

Table 2
Behavioral variant FTD–related pattern classification results

Subjects (N)	Sensitivity%	95% CI	Specificity%	95% CI	AUC%	95% CI
bvFTD (59) *versus*						
NL (30)	91.5 (54/59)	81.3-97.2	93.3 (28/30)	77.9-99.2	97.7	92-99.7
AD (50)	91.5 (54/59)	81.3-97.2	82 (41/50)	68.6-91.4	92.2	85.4-96.4
FTD language variants* (29)	71.2 (42/59)	57.9-82.2	86.2 (25/29)	68.3-96.1	87.6	78.8-93.6

Abbreviations: AD, Alzheimer's disease; AUC, area under the receiver operating characteristics curve; bvFTD, behavioral variant frontotemporal dementia; CI, confidence interval; NL, healthy controls.

NOTE. Parentheses contain numbers of subjects.

*Including 12 patients with progressive nonfluent aphasia and 17 patients with semantic dementia.

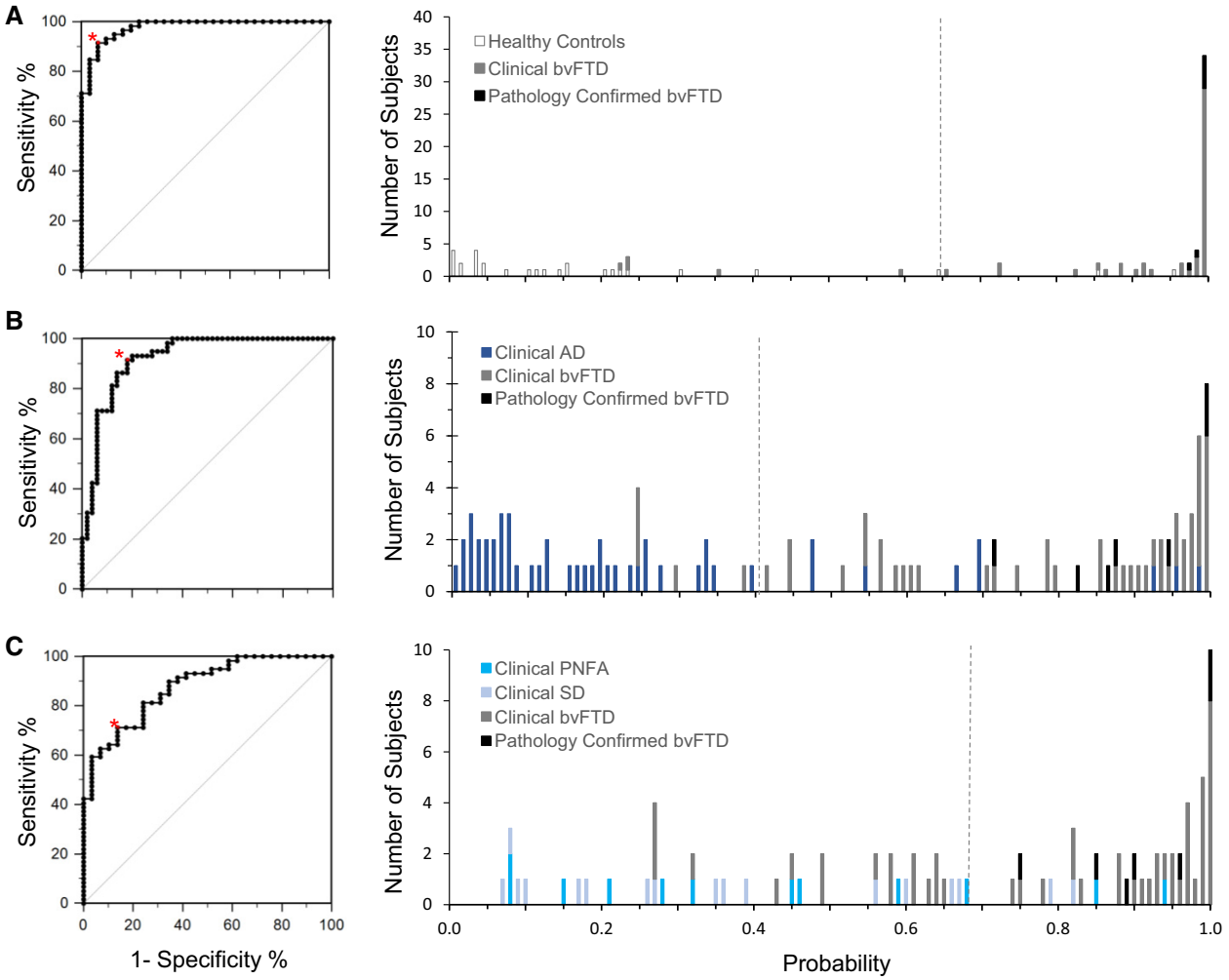

Fig. 4. Single-case classifications: Single-case classification analyses were performed in combined testing data from all sites. For each classification (A: bvFTD versus healthy controls; B: bvFTD versus AD; and C: bvFTD versus language variants of FTD, i.e., PNFA and SD), a cutoff point (indicated by the red asterisk on each ROC curve, *left*) was determined based on optimal sensitivity/specificity values (cf. Section 2.6 and Table 2). The dashed line on each distribution plot (*right*) demonstrates the corresponding cutoff value for the predicted probability of bvFTD (Each unit bar represents an individual testing subject). Abbreviations: AD, Alzheimer's disease; ADNI, Alzheimer's Disease Neuroimaging Initiative; bvFTD, behavioral variant frontotemporal dementia; NL, healthy controls; PNFA, progressive nonfluent aphasia; SD, semantic dementia.

92.2% ($P < .0001$; logistic regression; see Fig. 4B and Table 2), which slightly decreased when only subjects at early stage of the disease (31 bvFTD and 24 AD) were used in the analysis (area under the curve = 0.90, $P < .0001$; cf. Section 2.1). Classification between bvFTD and FTD language variants resulted in a discriminatory power of 87.6% ($P < .0001$; see Fig. 4C). Table 2 summarizes the performance of the aforementioned classification analyses.

3.3.3. Clinical correlates

The expression of bFDRP was elevated in subjects at the late stage of the disease (symptom duration > 3.5 years) compared with those at the early stage (symptom duration < 3.5 years) ($P = .035$; Student's *t*-test; Fig. 5, *right*). Similarly, bFDRP expression was elevated with increasing functional impairment as evaluated by CDR ($P = .008$, one-way ANOVA; $P < .05$, post hoc test; Fig. 5, *middle*). The bFDRP expression values correlated with CDR global scores (r = 0.5, $P < .01$, Spearman's rho) but not with years of symptom duration (r = 0.19, $P = .2$, Pearson's correlation). Of note, both the *early* and the *very mild* subgroups demonstrated significant elevation of bFDRP expression compared with the corresponding healthy control group ($P < .001$; Student *t*-tests).

3.4. Reproducibility

We identified an analogous bvFTD-related covariance pattern (i.e., $bFDRP_B$) in FDG PET data from the seven pathology-confirmed bvFTD patients and their age-matched healthy subjects scanned at Center-B (Table 1). The $bFDRP_B$ was represented by the first principal component (PC1 accounting for 43.3% of the subject × voxel variance), the only PC that could distinguish patients from

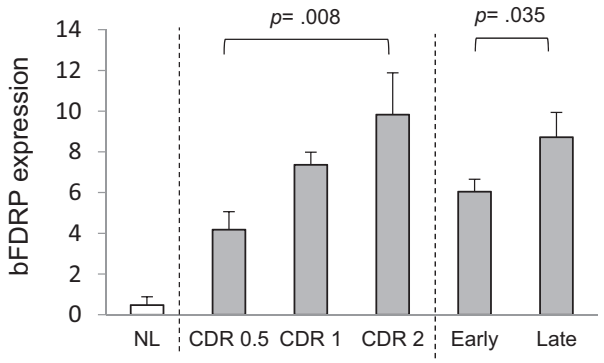

Fig. 5. Clinical correlates of bFDRP: Testing bvFTD data from Center-B were categorized based on severity of functional impairment using CDR (*very mild:* CDR = 0.5, n = 9; *mild*: CDR = 1, n = 21; and *moderate:* CDR = 2, n = 7) or disease stage using symptom duration (*early*: symptom duration < 3.5 years versus *late*: symptom duration > 3.5 years). *Left*: bFDRP expression in the NL group is shown for reference. The expression of bFDRP was elevated in both the *early* and *very mild* subgroups compared with NL ($P < .001$, Student *t*-tests). *Middle:* Expression values for the bFDRP increased with worsening functional impairment (F [2, 36] = 5.7, $P < .01$; one-way ANOVA), with significantly greater expression in patients with higher CDR values ($P < .05$; post hoc test). *Right*: The expression of bFDRP was greater in subjects at late stage of the disease compared with those at early stage ($P = .035$; Student's *t*-test). (Pattern expression was standardized to the reference group used for pattern identification). Abbreviations: bvFTD, behavioral variant frontotemporal dementia; bFDRP, behavioral variant frontotemporal dementia–related pattern; CDR, Clinical Dementia Rating; NL, healthy controls.

control subjects ($P < .001$; permutation test, 500 iterations; Fig. 6A). The expression of this pattern was elevated in testing bvFTD patients compared with corresponding healthy subjects scanned at each center ($P < .001$, for both centers, Student's *t*-tests; Fig. 6C). Like the pattern derived from Center-A data, $bFDRP_B$ was significantly more expressed in patients with more advanced disease as determined by CDR ($P = .014$, one-way ANOVA, $P < .05$, post hoc test; r = 0.46, $P < .01$, Spearman's rho) or symptom duration (*early* vs. *late,* $P = .02$, Student *t*-test) (see Supplementary Fig. 2).

The metabolic topography of this pattern, reported in Fig. 6B, was highly correlated with the one derived from Center-A data (r = 0.73, $P < .001$; voxelwise correlation corrected for autocorrelation [24]; Fig. 6D, *left*). We also observed a strong correlation between corresponding expression values for the two patterns measured in the testing bvFTD subjects (r = 0.97, $P < .001$, *Center-A and Center-B testing* groups combined; Pearson's correlations; Fig. 6D, *right*).

3.5. The topography of bFDRP

The topographies of bFDRP identified at the two sites (Fig. 2B and Fig. 6B) demonstrated covarying reductions in metabolic activity involving the anterior cingulate, medial prefrontal, and orbitofrontal cortices; middle and inferior frontal gyri; superior temporal gyrus; insula; and thalamus, accompanied by relative metabolic increases in the middle and inferior occipital gyri. The reliability of voxel weights in the aforementioned regions were ascertained by bootstrap estimation, with absolute values for the ICV map (|z|) greater than 1.64 ($P < .05$, one-tailed; 500 iterations).

4. Discussion

This study identified the metabolic covariance pattern associated with bvFTD (i.e., bFDRP) from two independent sites and assessed its performance as a quantitative imaging marker in clinically as well as pathology-confirmed bvFTD subjects. The single-case quantification of bFDRP showed significant clinical correlates and good-to-excellent classification between bvFTD and other dementias.

4.1. Validation of bFDRP as a bvFTD imaging marker

Expression values for bFDRP separated the testing bvFTD patients scanned at each site from the healthy controls with high sensitivity and specificity (>90%). Of note, all the eight pathology-confirmed bvFTD subjects, from both sites, were separated from the corresponding control subjects. The consistently elevated expression of bFDRP across independent bvFTD testing samples and the highly intercorrelated expression values of bFDRPs derived from the two sites point to the generalizability of bFDRP across scanners and populations [10]. Furthermore, our cross-sectional observation suggests that bFDRP expression associates with the disease progression, demonstrating its potential application as a disease-monitoring biomarker for bvFTD [26].

4.2. Performance of bFDRP in disease classifications

Automated quantification of bFDRP expression on a single-case basis allowed a discriminatory power of 92.2% and a sensitivity of 91.5% with specificity of 82% in distinguishing bvFTD from AD. That said, a direct numerical comparison with previous reports may be inconclusive due to differences in the characteristics of the research samples and the various measures used to determine early-stage dementia [3,27,28]. For instance, previous studies have merged language and behavioral variants of FTD into one group leading to a heterogeneous sample [22,27]. However, in this study, we observed that bFDRP could also distinguish bvFTD from language variants of FTD with about 71% sensitivity and 86% specificity. Moreover, in the absence of standardized clinical rating scales for bvFTD [29], most previous studies [27,28,30] have used general dementia rating scales (such as MMSE) to determine early or mild stages of bvFTD. However, these measures, commonly used for AD, do not consistently correlate with disease progression and the associated deterioration of social and behavioral symptoms in bvFTD, thus often underrating its severity [29,31,32].

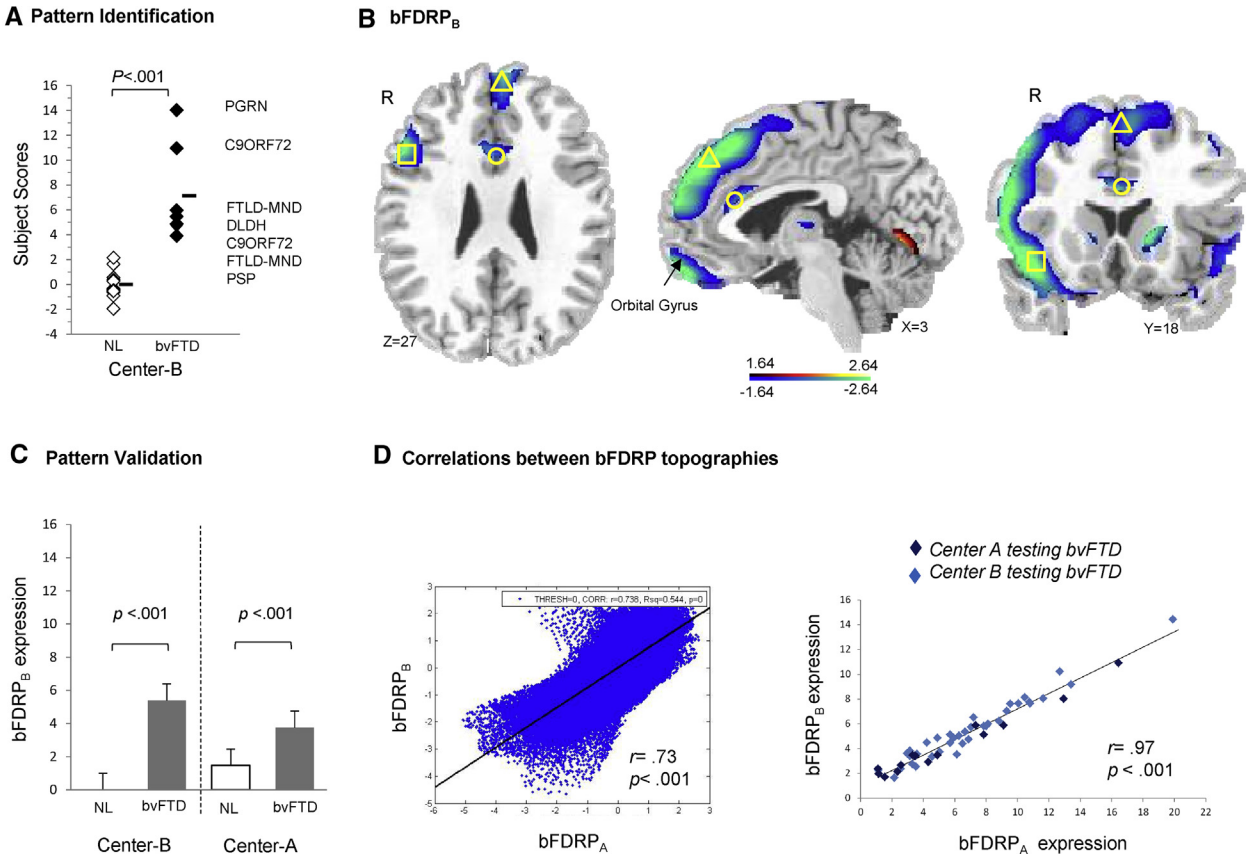

Fig. 6. Reproducibility of bFDRP: (A) Spatial covariance analysis (SSM/PCA) was performed on FDG PET scans from seven pathology-confirmed bvFTD patients and 15 age-matched healthy volunteers (NL) all scanned at Center-B. The confirmation of FTLD pathology was achieved either through genotyping or autopsy, as listed beside each corresponding data point. The first principal component, accounting for 43.3% of subject × voxel variance (cf. Supplementary Fig. 1), was the only principal component that could separate patients and NL ($P < .001$; permutation test) and was termed $bFDRP_B$ (Subjects scores are standardized to the Center-B reference group used for pattern identification [mean = 0; SD = 1]). (B) Similar to bFDRP derived from Center-A data, prominent metabolic reductions in the medial prefrontal (*triangle*), anterior cingulate (*circle*), and inferior frontal (*rectangle*) gyri were evident in the $bFDRP_B$ topography (The images are generated by superimposing the candidate topography onto a standard brain template. The displayed regions contributed significantly to the topography at $|z| > 1.64$, $P < .05$ [one-tailed], and demonstrated to be reliable by bootstrap estimation. Regions with positive weights [i.e., covariance metabolism above mean] were color-coded red, whereas those with negative weights [i.e., covariance metabolism below mean] were color-coded blue. The right hemisphere is labeled "R"). (C) The expression values of $bFDRP_B$ was found elevated in the scan data of independent bvFTD testing samples from each site when compared with the corresponding healthy control groups ($P < .001$, Student's *t*-test, for both sites; *left*: Center-B testing data; *right*: combined bvFTD and NL groups from Center-A) (Error bars represent standard error of the mean [SE] for each group. Subjects scores are standardized to the Center-B reference group used for pattern identification). (D) *Left:* The $bFDRP_B$ topography significantly correlated with the bFDRP identified at Center-A ($r = 0.73$, $P < .001$; voxelwise correlation corrected for spatial autocorrelation [23]). *Right:* Similarly, a strong correlation was observed between the expression values of the two bFDRP topographies in all testing bvFTD subjects ($r = 0.97$, $P < .001$; Pearson Correlation). Abbreviations: bvFTD, behavioral variant frontotemporal dementia; bFDRP, behavioral variant frontotemporal dementia–related pattern; *C9ORF72*, chromosome 9 open reading frame 72 hexanucleotide repeat expansion; DLDH, dementia lacking distinctive histopathological features; FTLD, frontotemporal lobar degeneration; FTLD-MND, frontotemporal lobar degeneration–motor neuron degeneration; *PGRN*, progranulin mutation; PSP, FTLD histopathology consistent with progressive supranuclear palsy; NL, healthy controls; PCA, principal component analysis; SSM, scaled subprofile modeling.

To overcome this limitation, we used symptom duration as the main metric to identify subjects at the early stage of dementia [29]; and general cognitive measures were only used to exclude subjects with early presentation of marked cognitive or functional impairment [29]. This staging approach appears to be more valid than a sole reliance on general cognitive measures for comparing between bvFTD and AD [33,34]. In this regard, the bFDRP classification power between early-stage bvFTD and AD subjects slightly decreased to 90.1%; that said, a high specificity (83.3%) was retained with a relative decline in sensitivity (83.8%). This apparent increase in misclassification may be due to the higher rate of clinical misdiagnosis between the two dementias at earlier stages of the disease.

4.3. The topography of bFDRP

The regional involvement revealed by this study's multivariate method corroborated the univariate findings reported in several independent cohorts of bvFTD patients [3,35–37],

including hypometabolism in insular, medial prefrontal, and anterior cingulate cortices as well as thalamus. Of note, a progressive disruption of white matter connections between medial prefrontal and anterior cingulate cortices has recently been reported in bvFTD patients [38], further highlighting the integrated role of these regions in bvFTD pathomechanism. The data-driven results presented in this study are also in line with the reduced functional connectivity of orbital frontoinsular and dorsal anterior cingulate cortex (the key regions involved in salience processing [39]) previously reported in bvFTD patients [40–42].

In addition, we noted relative metabolic increases in the middle and inferior occipital gyri as part of the bFDRP topography. SPECT imaging has disclosed analogous increases in resting occipital lobe perfusion in FTD [43]. These regional changes may be derived from reduction in the activity of inhibitory projections to this region from anterior temporal and frontal cortices, major areas of neurodegeneration in FTD [43], and have been associated with enhanced or emergent artistic skills observed in these patients [43].

That said, we observed slight regional discrepancies between the topographies derived from Center-A and Center-B data, including a more prominent thalamic hypometabolism in the Center-A–derived topography, and a more prominent orbitofrontal hypometabolism and a generally more asymmetric pattern in the Center-B–derived topography. These discrepancies may be in part due to different distribution of underlying pathology between the two derivational groups. While the underlying pathology for most subjects enrolled at Center-B derivational group was consistent with TDP-43 pathology (cf. Fig. 6A), the underlying pathology for the Center-A derivational group was generally unknown (except for the one TDP-43 autopsied case). Nonetheless, the expression values for both disease-related topographies were highly intercorrelated in testing bvFTD patients from the two sites.

4.4. Technical considerations and practical applications

To assess the generalizability of bFDRP, we treated data from the two sites independently both at identification and validation levels. By not mixing the data from the two sites, we also avoided introduction of site-related confounding variables, such as hardware and software discrepancies, in data covariance. The effect of such variables was further minimized by using the corresponding healthy controls from each site for the aforementioned analyses.

A limitation of this retrospective study was that brain MRI scan was not broadly accessible for all subjects, thus the characterization of the bvFTD metabolic covariance pattern could not include volumetric measures. Of note, in neurodegenerative processes, the synaptic failure and concomitant reduction in local metabolic activity precedes neuronal death and the consequent volume loss. In fact, at early stages of neurodegeneration, localized metabolic reductions were reported in the absence of considerable atrophy [44,45].

Another limitation of this study was the lack of longitudinal data to explore the relationship between bFDRP expression values and disease progression. In the absence of such data, we had to rely on symptom duration, as a cross-sectional measure of disease progression. Owing to the heterogeneous nature of bvFTD and the inherent variety in the patients' progression rates, this approach may have underestimated the true relationship between bFDRP expression and the underlying disease progression. Future longitudinal studies are required to appropriately investigate the potential of bFDRP as a disease-monitoring biomarker.

In addition, although a nonelevated bFDRP expression could exclude bvFTD with high likelihood, the determination of alternative diagnoses will require a multipattern approach that concurrently takes into account the covariance patterns of other diagnostic categories [46]. This approach will also allow the identification of indeterminate subjects, further increasing the specificity of differential diagnosis, which would be particularly useful in the settings of sample selection for clinical drug trials.

Finally, the present study used a data-driven, voxel-based multivariate methodology [13,14,26] to identify the covariance pattern associated with bvFTD (i.e., bFDRP), which has not been determined before. This methodology is known to detect early neurodegenerative changes with greater accuracy than univariate or "region-of-interest" approaches [26]. Notably, the forward quantification of bFDRP expression in an individual patient scan does not rely on any *a priori* regional measurement; instead, it reflects the holistic interregional covariance of voxel deviation from reference mean values of FDG uptake [14]. Hence, the single-case measurements are minimally affected by the individual variability in regional involvement. This feature is specifically important in development of quantitative imaging biomarkers for a pathologically and neuroanatomically heterogeneous disorder like bvFTD [1,6,8].

Acknowledgments

The authors wish to thank Dr. Mark Gudesblatt and Dr. Philip Ragone for their help in patient selection and clinical evaluation. The authors are grateful to the staff of the Cyclotron and PET facility at The Feinstein Institute for Medical Research for helping with the imaging studies, to Drs. Maja Trost, Katharina Schindlbeck, and Vicky Brandt for critical reading of the manuscript, and to Ms. Yoon Young Choi and Ms. Toni Fitzpatrick for their assistance in manuscript preparation.

This work was supported in part by the National Institute of Neurological Disorders and Stroke (P50 NS071675 [Morris

K. Udall Center of Excellence for Parkinson's Disease Research at The Feinstein Institute for Medical Research] to D.E.). Some of data used in this study were obtained from Alzheimer's Disease Neuroimaging Initiative (ADNI), funded by the National Institutes of Health (Grant U01 AG024904) and DOD ADNI (Department of Defense award number W81XWH-12-2-0012). A full list of ADNI funding is available here: http://adni.loni.usc.edu/about/funding/

Role of funder/sponsor: The content is solely the responsibility of the authors and does not necessarily represent the official views of the National Institute of Neurological Disorders and Stroke or the National Institutes of Health. The sponsor did not play a role in study design, collection, analysis or interpretation of data, writing the report, or in the decision to submit the article for publication.

Supplementary data

Supplementary data related to this article can be found at https://doi.org/10.1016/j.dadm.2018.07.009.

RESEARCH IN CONTEXT

1. Systematic review: Based on our literature review using conventional search engines (e.g., PUBMED.COM), previous studies have collectively revealed the brain regional patterns of neurodegeneration in behavioral variant frontotemporal dementia (bvFTD) using univariate or region-of-interest methods of image analysis. However, the neuroanatomical heterogeneity of bvFTD calls for multivariate imaging biomarkers for clinical applications.
2. Interpretation: A spatial covariance pattern of abnormal brain glucose metabolism, termed bFDRP (bvFTD-related pattern), can be used to quantify the early neurodegenerative changes related to bvFTD. As a quantitative imaging marker, bFDRP can facilitate the monitoring of disease progress in patients with bvFTD.
3. Future directions: Further research should investigate a multipattern approach for differential diagnosis of dementia syndromes. Longitudinal FDG PET studies should validate the application of bFDRP for disease monitoring and prognostication. Future investigations may discover pathology-specific metabolic topographies that can optimize sample selection in disease-modifying therapeutic trials of bvFTD.

References

[1] Bang J, Spina S, Miller BL. Frontotemporal dementia. Lancet 2015; 386:1672–82.
[2] Krudop WA, Dols A, Kerssens CJ, Eikelenboom P, Prins ND, Moller C, et al. The pitfall of behavioral variant frontotemporal dementia mimics despite multidisciplinary application of the FTDC criteria. J Alzheimers Dis 2017;60:959–75.
[3] Foster NL, Heidebrink JL, Clark CM, Jagust WJ, Arnold SE, Barbas NR, et al. FDG-PET improves accuracy in distinguishing frontotemporal dementia and Alzheimer's disease. Brain 2007; 130:2616–35.
[4] Rascovsky K, Hodges JR, Knopman D, Mendez MF, Kramer JH, Neuhaus J, et al. Sensitivity of revised diagnostic criteria for the behavioural variant of frontotemporal dementia. Brain 2011;134:2456–77.
[5] McKhann GM, Knopman DS, Chertkow H, Hyman BT, Jack CR Jr, Kawas CH, et al. The diagnosis of dementia due to Alzheimer's disease: recommendations from the National Institute on Aging-Alzheimer's Association workgroups on diagnostic guidelines for Alzheimer's disease. Alzheimers Dement 2011;7:263–9.
[6] Whitwell JL, Przybelski SA, Weigand SD, Ivnik RJ, Vemuri P, Gunter JL, et al. Distinct anatomical subtypes of the behavioural variant of frontotemporal dementia: a cluster analysis study. Brain 2009;132:2932–46.
[7] Womack KB, Diaz-Arrastia R, Aizenstein HJ, Arnold SE, Barbas NR, Boeve BF, et al. Temporoparietal hypometabolism in frontotemporal lobar degeneration and associated imaging diagnostic errors. Arch Neurol 2011;68:329–37.
[8] Cerami C, Dodich A, Lettieri G, Iannaccone S, Magnani G, Marcone A, et al. Different FDG-PET metabolic patterns at single-subject level in the behavioral variant of fronto-temporal dementia. Cortex 2016;83:101–12.
[9] Gordon E, Rohrer JD, Fox NC. Advances in neuroimaging in frontotemporal dementia. J Neurochem 2016;138:193–210.
[10] Woo CW, Chang LJ, Lindquist MA, Wager TD. Building better biomarkers: brain models in translational neuroimaging. Nat Neurosci 2017;20:365–77.
[11] Yakushev I, Drzezga A, Habeck C. Metabolic connectivity: methods and applications. Curr Opin Neurol 2017;30:677–85.
[12] Meeter LH, Kaat LD, Rohrer JD, van Swieten JC. Imaging and fluid biomarkers in frontotemporal dementia. Nat Rev Neurol 2017; 13:406–19.
[13] Niethammer M, Eidelberg D. Metabolic brain networks in translational neurology: concepts and applications. Ann Neurol 2012; 72:635–47.
[14] Spetsieris P, Ma Y, Peng S, Ko JH, Dhawan V, Tang CC, et al. Identification of disease-related spatial covariance patterns using neuroimaging data. J Vis Exp 2013;76:e50319.
[15] Eidelberg D. Metabolic brain networks in neurodegenerative disorders: a functional imaging approach. Trends Neurosci 2009; 32:548–57.
[16] Neary D, Snowden JS, Gustafson L, Passant U, Stuss D, Black S, et al. Frontotemporal lobar degeneration: a consensus on clinical diagnostic criteria. Neurology 1998;51:1546–54.
[17] Mattis PJ, Niethammer M, Sako W, Tang CC, Nazem A, Gordon ML, et al. Distinct brain networks underlie cognitive dysfunction in Parkinson and Alzheimer diseases. Neurology 2016;87:1925–33.
[18] Knopman DS, Roberts RO. Estimating the number of persons with frontotemporal lobar degeneration in the US population. J Mol Neurosci 2011;45:330–5.
[19] Jost BC, Grossberg GT. The natural history of Alzheimer's disease: a brain bank study. J Am Geriatr Soc 1995;43:1248–55.
[20] Eckert T, Barnes A, Dhawan V, Frucht S, Gordon MF, Feigin AS, et al. FDG PET in the differential diagnosis of parkinsonian disorders. Neuroimage 2005;26:912–21.

[21] Diehl-Schmid J, Grimmer T, Drzezga A, Bornschein S, Riemenschneider M, Forstl H, et al. Decline of cerebral glucose metabolism in frontotemporal dementia: a longitudinal 18F-FDG-PET-study. Neurobiol Aging 2007;28:42–50.
[22] Perani D, Della Rosa PA, Cerami C, Gallivanone F, Fallanca F, Vanoli EG, et al. Validation of an optimized SPM procedure for FDG-PET in dementia diagnosis in a clinical setting. NeuroImage Clin 2014;6:445–54.
[23] Spetsieris PG, Eidelberg D. Scaled subprofile modeling of resting state imaging data in Parkinson's disease: methodological issues. Neuroimage 2011;54:2899–914.
[24] Ko JH, Spetsieris P, Ma Y, Dhawan V, Eidelberg D. Quantifying significance of topographical similarities of disease-related brain metabolic patterns. PLoS One 2014;9:e88119.
[25] Youden WJ. Index for rating diagnostic tests. Cancer 1950;3:32–5.
[26] Habeck C, Foster NL, Perneczky R, Kurz A, Alexopoulos P, Koeppe RA, et al. Multivariate and univariate neuroimaging biomarkers of Alzheimer's disease. Neuroimage 2008;40:1503–15.
[27] Titov D, Diehl-Schmid J, Shi K, Perneczky R, Zou N, Grimmer T, et al. Metabolic connectivity for differential diagnosis of dementing disorders. J Cereb Blood Flow Metab 2017;37:252–62.
[28] Mosconi L, Tsui WH, Herholz K, Pupi A, Drzezga A, Lucignani G, et al. Multicenter standardized 18F-FDG PET diagnosis of mild cognitive impairment, Alzheimer's disease, and other dementias. J Nucl Med 2008;49:390–8.
[29] Mioshi E, Hsieh S, Savage S, Hornberger M, Hodges JR. Clinical staging and disease progression in frontotemporal dementia. Neurology 2010;74:1591–7.
[30] Moller C, Pijnenburg YA, van der Flier WM, Versteeg A, Tijms B, de Munck JC, et al. Alzheimer disease and behavioral variant frontotemporal dementia: Automatic classification based on cortical atrophy for single-subject diagnosis. Radiology 2016;279:838–48.
[31] Tan KS, Libon DJ, Rascovsky K, Grossman M, Xie SX. Differential longitudinal decline on the Mini-Mental State Examination in frontotemporal lobar degeneration and Alzheimer disease. Alzheimer Dis Assoc Disord 2013;27:310–5.
[32] Knopman DS, Weintraub S, Pankratz VS. Language and behavior domains enhance the value of the clinical dementia rating scale. Alzheimers Dement 2011;7:293–9.
[33] Pasquier F, Richard F, Lebert F. Natural history of frontotemporal dementia: comparison with Alzheimer's disease. Dement Geriatr Cogn Disord 2004;17:253–7.
[34] Rosen HJ, Narvaez JM, Hallam B, Kramer JH, Wyss-Coray C, Gearhart R, et al. Neuropsychological and functional measures of severity in Alzheimer disease, frontotemporal dementia, and semantic dementia. Alzheimer Dis Assoc Disord 2004;18:202–7.
[35] Diehl J, Grimmer T, Drzezga A, Riemenschneider M, Forstl H, Kurz A. Cerebral metabolic patterns at early stages of frontotemporal dementia and semantic dementia. A PET study. Neurobiol Aging 2004;25:1051–6.
[36] Jeong Y, Cho SS, Park JM, Kang SJ, Lee JS, Kang E, et al. 18F-FDG PET findings in frontotemporal dementia: an SPM analysis of 29 patients. J Nucl Med 2005;46:233–9.
[37] Schroeter ML, Laird AR, Chwiesko C, Deuschl C, Schneider E, Bzdok D, et al. Conceptualizing neuropsychiatric diseases with multimodal data-driven meta-analyses - the case of behavioral variant frontotemporal dementia. Cortex 2014;57:22–37.
[38] Mahoney CJ, Simpson IJ, Nicholas JM, Fletcher PD, Downey LE, Golden HL, et al. Longitudinal diffusion tensor imaging in frontotemporal dementia. Ann Neurol 2015;77:33–46.
[39] Seeley WW, Menon V, Schatzberg AF, Keller J, Glover GH, Kenna H, et al. Dissociable intrinsic connectivity networks for salience processing and executive control. J Neurosci 2007;27:2349–56.
[40] Zhou J, Greicius MD, Gennatas ED, Growdon ME, Jang JY, Rabinovici GD, et al. Divergent network connectivity changes in behavioural variant frontotemporal dementia and Alzheimer's disease. Brain 2010;133:1352–67.
[41] Agosta F, Sala S, Valsasina P, Meani A, Canu E, Magnani G, et al. Brain network connectivity assessed using graph theory in frontotemporal dementia. Neurology 2013;81:134–43.
[42] Filippi M, Agosta F, Scola E, Canu E, Magnani G, Marcone A, et al. Functional network connectivity in the behavioral variant of frontotemporal dementia. Cortex 2013;49:2389–401.
[43] Miller BL, Cummings J, Mishkin F, Boone K, Prince F, Ponton M, et al. Emergence of artistic talent in frontotemporal dementia. Neurology 1998;51:978–82.
[44] Chetelat G, Desgranges B, Landeau B, Mezenge F, Poline JB, de la Sayette V, et al. Direct voxel-based comparison between grey matter hypometabolism and atrophy in Alzheimer's disease. Brain 2008;131:60–71.
[45] Morbelli S, Ferrara M, Fiz F, Dessi B, Arnaldi D, Picco A, et al. Mapping brain morphological and functional conversion patterns in predementia late-onset bvFTD. Eur J Nucl Med Mol Imaging 2016;43:1337–47.
[46] Tang CC, Poston KL, Eckert T, Feigin A, Frucht S, Gudesblatt M, et al. Differential diagnosis of parkinsonism: a metabolic imaging study using pattern analysis. Lancet Neurol 2010;9:149–58.